



저작자표시-비영리-변경금지 2.0 대한민국

이용자는 아래의 조건을 따르는 경우에 한하여 자유롭게

- 이 저작물을 복제, 배포, 전송, 전시, 공연 및 방송할 수 있습니다.

다음과 같은 조건을 따라야 합니다:



저작자표시. 귀하는 원저작자를 표시하여야 합니다.



비영리. 귀하는 이 저작물을 영리 목적으로 이용할 수 없습니다.



변경금지. 귀하는 이 저작물을 개작, 변형 또는 가공할 수 없습니다.

- 귀하는, 이 저작물의 재이용이나 배포의 경우, 이 저작물에 적용된 이용허락조건을 명확하게 나타내어야 합니다.
- 저작권자로부터 별도의 허가를 받으면 이러한 조건들은 적용되지 않습니다.

저작권법에 따른 이용자의 권리는 위의 내용에 의하여 영향을 받지 않습니다.

이것은 [이용허락규약\(Legal Code\)](#)을 이해하기 쉽게 요약한 것입니다.

[Disclaimer](#)

공학석사 학위논문

Effect of preparation conditions of  
 $V_2O_5/TiO_2$  catalysts for selective  
catalytic reduction of  $NO_x$  with  $NH_3$

$V_2O_5/TiO_2$  촉매 제조 조건이  $NO_x$ 의  
암모니아 선택적 촉매 환원 반응에  
미치는 영향

2014년 2월

서울대학교 대학원

화학생물공학부

윤 승 희

# Abstract

## Effect of preparation conditions of $V_2O_5/TiO_2$ catalysts for selective catalytic reduction of $NO_x$ with $NH_3$

Seunghee Youn

Chemical and Biological Engineering

The Graduate School

Seoul National University

International Maritime Organization (IMO) announced Tier III taking effect from 2016 which regulates  $NO_x$  emitted from vessels. Marine SCR catalyst requires higher De $NO_x$  activity in the low temperature range comparing to automobile. In this study, I aimed at finding the optimum condition to prepare  $V_2O_5/TiO_2$  catalyst known as low temperature selective catalytic reduction catalysts by changing oxidation states in vanadium precursor

solution.  $V_2O_5$  catalysts supported by  $TiO_2$  (1, 3, 5 and 7 wt%) were prepared by applying wet impregnation method using three precursor solutions with different oxidation states ( $V^{3+}$ ,  $V^{4+}$  and  $V^{5+}$ ).

I utilized BET, ICP, XRD, Raman spectroscopy, UV–Vis DRS,  $H_2$  TPR and XPS to investigate the physicochemical properties of  $V_2O_5/TiO_2$  catalysts. Also,  $NH_3$ –SCR reaction test was performed for these catalysts.

It was found that  $V_2O_5/TiO_2$  catalysts prepared from the precursor solution of  $V^{3+}$  oxidation state (VT(3+)) has good activity over wide temperature range and produces the lowest concentration of  $N_2O$  during SCR reaction. The formation of highly coordinated polymeric vanadyl species on the sample attributes the high  $NO_x$  conversion and low production of  $N_2O$  of the VT(3+) catalyst.

Keywords :  $V_2O_5/TiO_2$ , Oxidation state, Vanadium precursor, De $NO_x$ ,  $NH_3$ –SCR

Student Number: 2012–20962

# Contents

Abstract .....	1
List of Tables .....	5
List of Figures .....	6
Chapter 1. Introduction .....	7
1.1. Background of selective catalytic reduction (SCR) .....	7
1.2. Objectives .....	11
Chapter 2. Experimental .....	13
2.1. Catalyst preparation .....	13
2.2. Catalyst characterization .....	15
2.2.1. BET .....	15
2.2.2. XRD .....	15
2.2.3. Raman spectrometer .....	15
2.2.4. H <sub>2</sub> TPR.....	16
2.2.5. UV–Vis DRS.....	16
2.2.6. XPS .....	16
2.3. NH <sub>3</sub> –SCR activity test .....	18
Chapter 3. Results and Discussion .....	20
3.1. Catalysts preparation .....	20
3.2. Textural and structural properties .....	22
3.3. Raman spectroscopy .....	25
3.4. UV–Vis DRS .....	28
3.5. H <sub>2</sub> TPR .....	30

3.6. XPS .....	34
3.7. NH <sub>3</sub> -SCR activity .....	38
Chapter 4. Conclusion .....	45
Reference .....	46
요약 (국문초록) .....	51

## List of Tables

Table 1. NO <sub>x</sub> regulations on vessel announced by International Maritime Organization (IMO) .....	12
Table 2. ICP analysis and textural properties measured by BET method of catalysts .....	23
Table 3. The relative surface concentration of V/Ti .....	37

# List of Figures

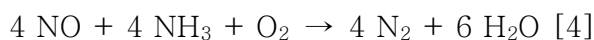
Figure 1. Selective catalytic reduction (SCR) system in diesel engine .....	9
Figure 2. Scheme of SCR reaction on $V_2O_5/TiO_2$ catalyst .....	10
Figure 3. Vanadium precursor solution with various oxidation states: $V^{3+}$ (left), $V^{4+}$ (center) and $V^{5+}$ (right) .....	14
Figure 4. XRD patterns of VT(3+) samples .....	24
Figure 5. Raman spectra of 7 wt% VT samples .....	27
Figure 6. UV-Vis spectra of (a) 5 wt% VT (b) 7wt% VT samples .....	29
Figure 7. $H_2$ TPR profile of VT(3+) samples with different vanadium loading .....	32
Figure 8. $H_2$ TPR profile of (a) 5 wt% VT (b) 7 wt% VT samples .....	33
Figure 9. V 2p XPS spectra of VT(3+) samples .....	36
Figure 10. $NO_x$ conversion of all VT samples .....	41
Figure 11. $NO_x$ conversion of 5 wt% VT samples .....	42
Figure 12. $N_2O$ concentration produced during SCR reaction of all VT samples .....	43
Figure 13. $N_2O$ concentration produced during SCR reaction of 5 wt% VT samples .....	44

# Chapter 1. Introduction

## 1.1. Background of selective catalytic reduction (SCR)

Nitrogen oxides (NO<sub>x</sub>) causes the photochemical smog, acid rain, ozone depletion and greenhouse effect. Therefore, a great deal of studies has been performed in the field of selective catalytic reduction (SCR) system. Recently, N<sub>2</sub>O has been focused due to its effect on greenhouse effect, known as having 310 times larger effect than CO<sub>2</sub> [1].

Selective catalytic reduction (SCR) of NO<sub>x</sub> by using NH<sub>3</sub> as a reductant (Figure 1) is a well-established and widely used process [2,3]. In general, it is accepted that the SCR of nitric oxide is based on the following reaction (Figure 2).

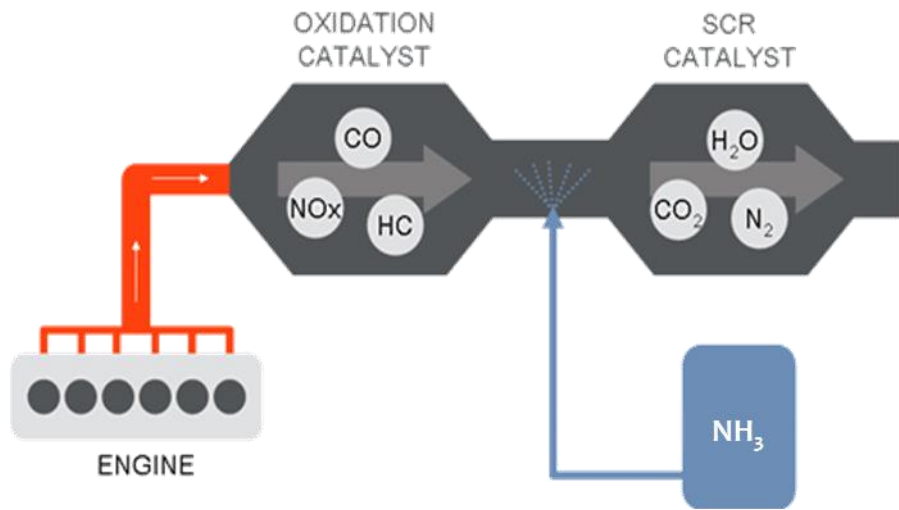


Several types of SCR catalysts have been reported, for example carbon-supported vanadia [5], copper oxides [6] and vanadia, chromia [7] supported on TiO<sub>2</sub>.

TiO<sub>2</sub> supported V<sub>2</sub>O<sub>5</sub> catalysts are widely used for the SCR of nitric oxide because of their high activity for nitric oxide

conversion in the presence of oxygen and their resistance to poisoning by sulfur dioxide [4,8].

The representative characteristics of vanadium used in  $V_2O_5/TiO_2$  catalyst is vanadium compounds have the  $V^{5+}$ ,  $V^{4+}$ ,  $V^{3+}$  and  $V^{0+}$  oxidation states theoretically. The wet impregnation method using vanadium precursor solution with  $V^{4+}$  oxidation state has been announced the most representative [9,10].  $V^{4+}$  is the most stable oxidation state of vanadium in acidic media so that lots of vanadium works largely spread on the reported values, especially for the  $V^{4+}$  and  $V^{3+}$  oxidation states [11].



Copyright © Castrol

Figure 1. Selective catalytic reduction (SCR) system in diesel engine.

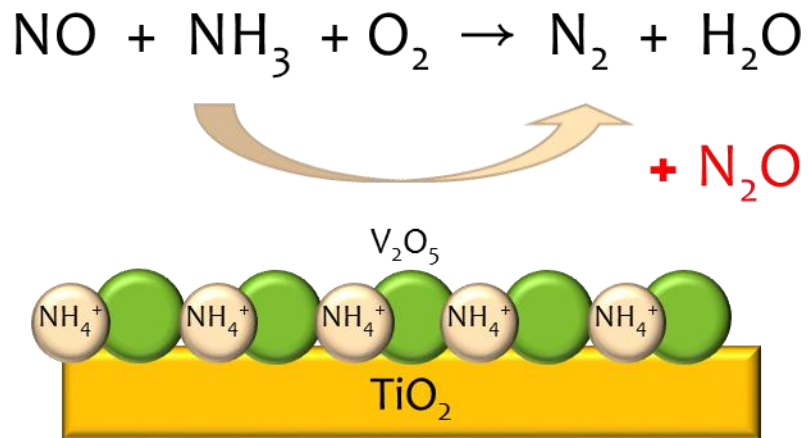


Figure 2. Scheme of SCR reaction on  $\text{V}_2\text{O}_5/\text{TiO}_2$  catalyst.

## 1.2. Objectives

In addition to the traditional NO<sub>x</sub> regulations on mobile or stationary sources, International Maritime Organization (IMO) announced the most stringent NO<sub>x</sub> regulations on vessel, Tier III, which will take effect from 2016 [12].

Especially, the SCR catalyst for marine application requires higher deNO<sub>x</sub> activity in the low temperature range due to the characteristics of marine exhaust. A low temperature SCR system has advantage of consuming less energy, thus having economic benefits [13]. The emission of NO<sub>x</sub> from vessel must be reduced approximately by 75% compared with 2011 (Table 1).

In addition to the low temperature deNO<sub>x</sub> activity, to our knowledge, there is no study about the effect of oxidation states of vanadium precursor solution on the V<sub>2</sub>O<sub>5</sub>/TiO<sub>2</sub> SCR catalysts.

Therefore, the aim of this study is to observe the effect of oxidation states of vanadium precursor solution on the V<sub>2</sub>O<sub>5</sub>/TiO<sub>2</sub> selective catalytic reduction catalyst. SCR reaction was monitored by using NO<sub>x</sub> analyzer and gas phase FT-IR to quantify the concentration of outlet gases. To analyze physicochemical properties of V<sub>2</sub>O<sub>5</sub>/TiO<sub>2</sub> catalysts, I employed several characterization methods, N<sub>2</sub> adsorption-desorption with BET method, ICP, XRD, Raman spectroscopy, XPS, UV-Vis and H<sub>2</sub> TPR.

Table 1. NOx regulations on vessel announced by International Maritime Organization (IMO).

Tier	Ship construction date on or after	Total weighted cycle emission limit (g/kWh) n = engine' s rated speed (rpm)		
		n < 130	n = 130 – 1999	n ≥ 2000
I	1 January 2000	17.0	$45.n^{-0.2}$	9.8
II	1 January 2011	14.4	$44.n^{-0.23}$	7.7
III	1 January 2016	3.4	$9.n^{-0.2}$	2.0

## Chapter 2. Experimental

### 2.1. Catalysts preparation

I used mesoporous anatase  $\text{TiO}_2$  powder (DT-51 Millennium Chemicals) as support of all catalysts. The wet impregnation method was implied to produce  $\text{VO}_x/\text{TiO}_2$  catalysts [14-18]. Ammonium metavanadate ( $\text{NH}_4\text{VO}_3$ ) (99% Sigma Aldrich) in oxalic acid and diluted water was used as precursor solution of catalysts. I controlled pH of the solution by adding oxalic acid to adjust the oxidation states of vanadium precursor. The color change of mixed precursor solution was observed in accordance with the oxidation states of vanadium [19,20]. As shown in Figure 3, each color of solution indicated the oxidation states: Yellow ( $\text{V}^{5+}$ ), Blue ( $\text{V}^{4+}$ ) and Green ( $\text{V}^{3+}$ ). After impregnation step, wet catalysts extracted from a rotary evaporator were dried overnight at  $105^\circ\text{C}$  and calcined at  $400^\circ\text{C}$  for 4h in air [14]. Sample was designated as the following notation X wt% VT(Y+), for example, 5 wt% VT(3+) meant 5 wt% of vanadium on  $\text{V}_2\text{O}_5/\text{TiO}_2$  catalysts starting from vanadium precursor solution of  $\text{V}^{3+}$ .



Figure 3. Vanadium precursor solution with various oxidation states:  $V^{3+}$  (left),  $V^{4+}$  (center) and  $V^{5+}$  (right).

## 2.2. Catalysts characterization

### 2.2.1. BET

Brunauer–Emmett–Teller (BET) method was applied to investigate the specific surface area of catalysts from N<sub>2</sub> adsorption isotherm at –196°C using ASAP 2010 (Micromeritics) apparatus. The samples about 0.4 g were degassed in flowing N<sub>2</sub> at 200°C for more than 12 h before measurement.

### 2.2.2. XRD

X–ray Diffractometer (XRD) patterns were confirmed by Ultra X18 (Rigaku) under 40 kV and 200 mA condition employing Cu K $\alpha$  radiation. From XRD patterns I obtained the crystallinity of the catalysts.

### 2.2.3. Raman spectrometer

Raman spectrometer, T64000 (HORIBA Jobin Yvon) is applied to investigate the metal oxides of each catalyst. The band placed at 520 cm<sup>-1</sup> (TiO<sub>2</sub>) was used to calibrate the Raman spectra. All VT samples were measured with a power of 110 mW and 50 mW for raw TiO<sub>2</sub> support. All samples including TiO<sub>2</sub> support were measured within same Raman shift.

#### 2.2.4. H<sub>2</sub> TPR

The reducibility of metal oxides was measured by H<sub>2</sub> TPR with a thermal conductivity detector (TCD) in a BEL-CAT-BASIC (BEL Japan Inc.). Prior to analysis procedure, 0.03 g samples were pretreated at 350°C for 1 h in a flow of 30 ml/min Ar. After cooling down to room temperature, then samples were exposed to 5% H<sub>2</sub>/Ar until the temperature reached 750°C at the rate of 10°C/min. During temperature programmed process, I could calculate the amount of hydrogen consumption and this data.

#### 2.2.5. UV-Vis DRS

The UV-Vis DRS spectra of V<sub>2</sub>O<sub>5</sub>/TiO<sub>2</sub> catalysts were recorded on a Jasco V-670 spectrometer. The catalytic characterization with UV-Vis DRS was performed at room temperature in air and spectra were obtained in the range of 190–1000 nm wavelength at the scanning speed of 1000 nm/min.

#### 2.2.6. XPS

The oxidation state of vanadium species was analyzed by X-ray Photoelectron Spectroscopy (XPS). Furthermore, the relative surface concentration of V/Ti on catalysts was gained by comparing the area of XPS spectra of each element. The XPS analyses were conducted on a MultiLab ESCA 2000 X-ray photoelectron spectrometer with Mg K  $\alpha$  radiation at 300 W. The catalysts were degassed overnight at room temperature and

pressures on the order of  $10^{-7}$  torr. The effects of the sample charging were eliminated by correcting the observed spectra for a C 1s binding energy value of 284.6 eV.

### 2.3. NH<sub>3</sub>–SCR activity test

Prior to the activity test, all catalyst samples were sieved into 300–500  $\mu\text{m}$ . 0.15 g sieved catalyst samples were loaded in a fixed-bed quartz tubular reactor to carry out SCR activity measurements. I raised reaction temperature from 150°C to 400°C and analyzed outlet gas at every 50°C. The composition of inlet reactant gas was 500 ppm NO, 500 ppm NH<sub>3</sub>, 2% O<sub>2</sub> and balanced with N<sub>2</sub>. Space velocity of inlet gas was determined to be 40,000 h<sup>-1</sup>.

After passing through a series of mass flow controllers which controlled flow of individual gas, all gaseous reactants were introduced to Fourier Transform Infrared (FT–IR) spectroscopy added to observe the concentration of NH<sub>3</sub> and N<sub>2</sub>O. A Nicolet 6700 (Thermo Scientific) with 2 m gas analysis cell heated to 80° C, was used for gas phase analysis. Data was averaged using 16 scans at a resolution of 1.0 cm<sup>-1</sup>. The calibration curves of NH<sub>3</sub> and N<sub>2</sub>O were obtained by using 5 calibration points of standard gas concentration acquired from FT–IR spectra.

Afterward, gas entered into Model 42i High level (Thermo Scientific) NOx chemiluminescence analyzer which was applied to measure NOx concentration of outlet gas.

The efficiency of activity test was discussed with NOx conversion provided from NOx analyzer and  $[\text{N}_2]_{\text{produced}}$  obtained by using the following equation.

$$\begin{aligned} & [\text{N}_2]_{\text{produced}} \\ &= \frac{1}{2} \times [ [\text{NO}_x]_{\text{In}} - [\text{NO}_x]_{\text{Out}} + [\text{NH}_3]_{\text{In}} - [\text{NH}_3]_{\text{Out}} - 2 \times [\text{N}_2\text{O}]_{\text{Out}} ] \end{aligned}$$

## Chapter 3. Result and Discussion

### 3.1. Catalysts preparation

Transition metal exhibits multiple oxidation states. Vanadium which is used as an active metal of our catalysts is also known as a transition metal having various oxidation states from  $V^{5+}$  to  $V^{2+}$ . Diverse oxidation states of vanadium ions can be distinguished by their unique colors. I prepare vanadium precursor solution exhibiting different colors as shown in Figure 3. During the process of preparing vanadium precursor solution and wet impregnation in a rotary evaporator, I can observe the different colors of vanadium precursor. The change in colors of vanadium precursor solution implies the formation of various oxidation states of vanadium species from 5+ to 3+.

According to the previous reports, vanadium oxide exhibiting different oxidation states exist as different forms in oxalic acid solution.  $V^{5+}$  exists in the form of  $VO_2(Ox)^-$  with yellow color in oxalic acid solution designated as  $H_2Ox$  ( $Ox: C_2O_4^{2-}$ ) [21,22]. When pH decreases with adding oxalic acid, the color of these  $V^{5+}$  compounds are reduced to  $V^{4+}$  existing as  $VO(Ox)_2^{2-}$  observed as blue solution [23]. Furthermore,  $V^{4+}$  is reduced to  $V^{3+}$  with green-colored solution of the form of  $VO_2(Ox)_2^{3-}$  as more oxalic acid added [24].

As a result, I could obtain the various vanadium precursor solution with different oxidation states of vanadium from 5+ to 3+ by controlling the pH of each vanadium precursor solution. Each pH of existence of specified vanadium oxide is as followed: 1.62 ( $V^{5+}$ ), 1.35 ( $V^{4+}$ ) and 0.86 ( $V^{3+}$ )

## 3.2. Textural and structural properties

The BET surface area and pore volume results are summarized in Table 2. Increment of vanadium loading on TiO<sub>2</sub> support causes decrease in surface area and pore volume of samples. However, no significant difference is observed in textural properties depending on the oxidation states of vanadium precursor solution. I confirmed the amount of vanadium in the sample from the ICP analysis, as summarized also in Table 2.

Figure 4 shows XRD patterns of VT(3+) samples with various vanadium loadings. XRD patterns demonstrate only peaks assigned to anatase TiO<sub>2</sub> phase. No peak assigned to vanadium oxide is shown on XRD patterns even in the highest vanadium loading sample, 7 wt% VT, indicating that no crystalline V<sub>2</sub>O<sub>5</sub> phase is formed. Irrespective of the oxidation state of vanadium precursor solution, all other samples with different oxidation states also demonstrate the same XRD patterns. The fact that no XRD peaks assigned to vanadium species are observed implies that vanadium oxides are well dispersed on TiO<sub>2</sub>.

Table 2. ICP analysis and textural properties measured by BET method of catalysts.

Sample		V (wt%) (ICP)	Specific surface area (m <sup>2</sup> /g)	Pore volume (cm <sup>3</sup> /g)
TiO <sub>2</sub> (Support)		–	82	0.30
VT(3+)	1wt%	1.08	82	0.32
	3wt%	3.30	76	0.29
	5wt%	5.00	74	0.26
	7wt%	8.02	69	0.24
VT(4+)	1wt%	0.99	83	0.29
	3wt%	2.71	77	0.27
	5wt%	5.51	71	0.24
	7wt%	8.12	68	0.21
VT(5+)	1wt%	1.06	84	0.29
	3wt%	2.99	76	0.26
	5wt%	5.57	66	0.24
	7wt%	8.27	57	0.21

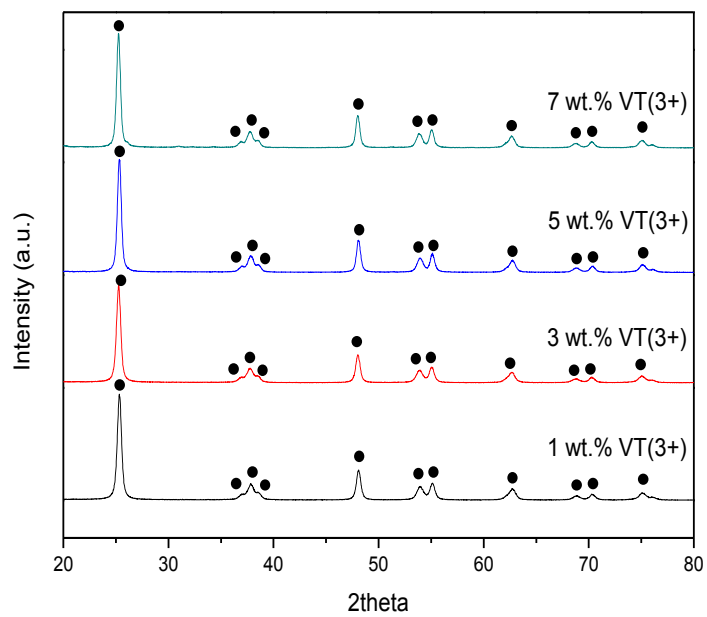


Figure 4. XRD patterns of VT(3+) samples.

### 3.3. Raman spectroscopy

No evidence of structural differences among various samples is found from XRD results, since vanadium species do not arise on XRD patterns. Raman spectra, known to be highly sensitive to observe the V=O vibration in vanadium oxides, was taken for various VT samples.

At 900–1000  $\text{cm}^{-1}$  in Raman shifts, the band of the terminal V=O bond of monomeric vanadium and polymeric vanadium species appears [25,26]. I can observe bulk vanadium is prevalently discovered around 1030  $\text{cm}^{-1}$  in low concentration of  $\text{V}_2\text{O}_5$ , resulting from very strong V=O bond [27]. With increasing vanadium loading, new Raman band around 800–1000  $\text{cm}^{-1}$  appears which attributes to the terminal V=O bonds of polymeric vanadium oxide species [26,28].

Although samples with vanadium loading from 1 wt% to 5 wt% VT samples do not show any Raman spectra, all 7 wt% VT samples show a peak assigned to polymeric vanadium species in Raman spectra between 980 and 1000  $\text{cm}^{-1}$  (Figure 5) [29, 30]. However, there is a slight difference in the location of the peak originating from polymeric vanadyl band. The peak of 7 wt% VT(3+) sample appears at 1000  $\text{cm}^{-1}$  and the one of 7 wt% VT(4+) presents at 985  $\text{cm}^{-1}$ , respectively. Increment of vanadium coordination and amount of polyvanadate species causes the shift of the band to higher Raman shift [26]. Therefore, Raman result confirms that VT(3+) samples tend to

form more highly coordinated polymeric vanadium species than VT(4+) samples based on the shift of the V=O band to higher Raman shift. In addition, 7 wt% VT(5+) catalyst also contain vanadium species with higher coordination than 7 wt% VT(4+) catalyst. This means the coordination number increases as following order: VT(3+) > VT(5+) > VT(4+)

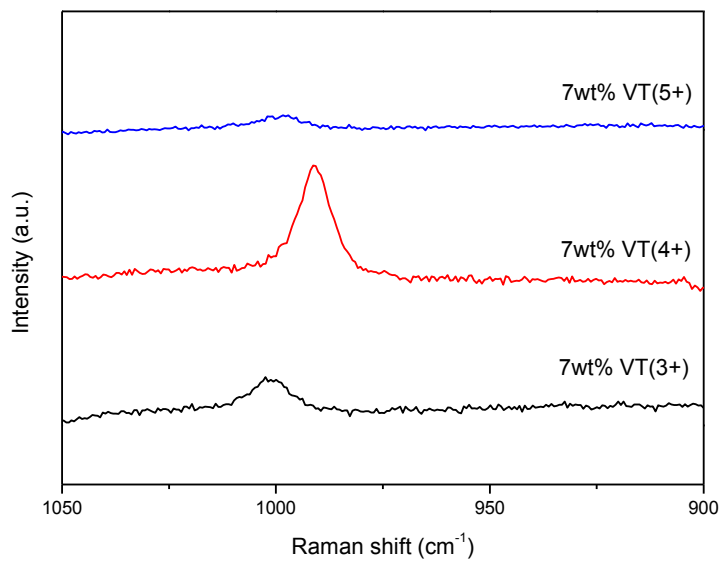


Figure 5. Raman spectra of 7 wt% VT samples.

### 3.4. UV–Vis DRS

UV–Vis DRS is a powerful tool to elucidate the structure and types of vanadia species present in  $V_2O_5/TiO_2$  catalysts.  $TiO_2$  support absorbs in the UV region of 320–350 nm [29,30], while the absorption band of  $V_2O_5$  oxides largely expands to the visible region [29,31]. The coordination structure of vanadium oxide species has significant effect on UV–Vis adsorption edge position of  $V_2O_5/TiO_2$ . In other words, the formation of the highly coordinated polymeric vanadium species appears the higher adsorption edge wavelength [32].

Figure 6(a) shows the UV–Vis absorption edge positions of 5 wt%  $V_2O_5/TiO_2$  catalyst. The edge position decreases from 550 nm to 523 nm in order of VT(3+), VT(5+) and VT(4+), suggesting that VT(3+) samples contain the highest polymerization degree than other oxidation state samples. As demonstrated in Figure 6(b), the UV–Vis absorption edge of three 7 wt% VT samples follow the same trend. It can be generalized that VT(3+) samples produced the highest polymerized vanadia species. Especially, it must be pointed out that the order of polymerized vanadium oxides in these UV–Vis results are well corresponding to Raman results, as determined by the peak position of V=O band in Figure 5 [32]. To sum up, both Raman and UV–Vis results support the formation of highly polymerized vanadium species on VT(3+) samples.

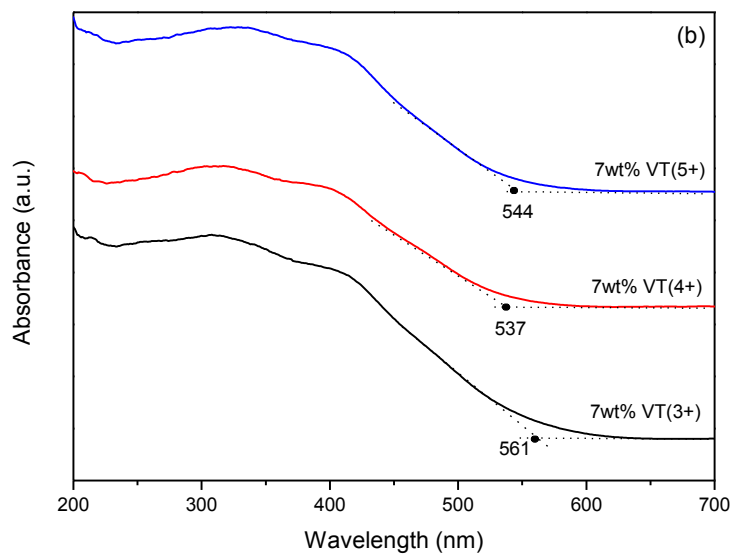
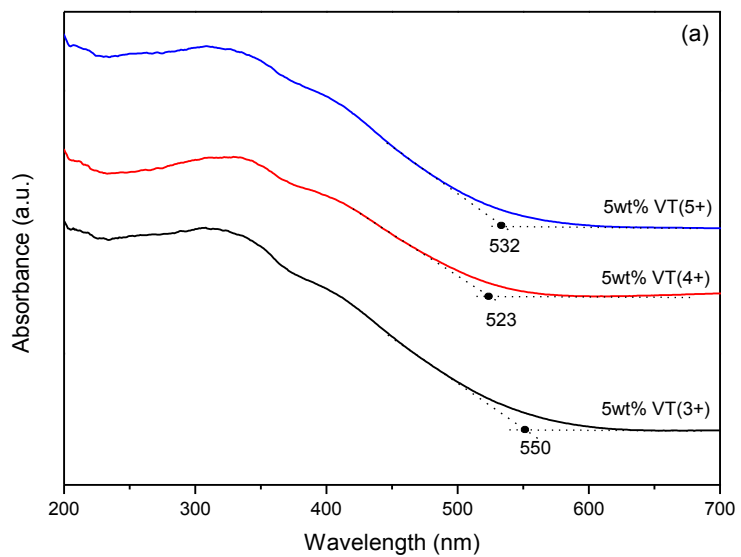


Figure 6. UV-Vis spectra of (a) 5 wt% VT (b) 7 wt% VT samples.

### 3.5. H<sub>2</sub> TPR

H<sub>2</sub> TPR results inform the reduction behavior of vanadia species [33–35]. It was reported that bulk vanadium oxide reduces at much higher temperature over 700°C than supported vanadium oxide. Therefore, the appearance of reduction peak at low temperature around 400–500°C is due to the surface vanadium oxide, while high temperature peak is assigned to the reduction of bulk vanadium oxide [36]. Reduction peaks at 692, 730 and 794 °C originate from the reduction from V<sub>2</sub>O<sub>5</sub> to V<sub>6</sub>O<sub>13</sub>, V<sub>2</sub>O<sub>4</sub> and V<sub>2</sub>O<sub>3</sub>, respectively. Such high temperature peak arises from bulk vanadia reduction [35] In this study, I cannot find any reduction peak above 700°C, indicating that vanadia species in this study are well dispersed on TiO<sub>2</sub>. This result indicates that H<sub>2</sub> TPR and XRD results are in good agreement.

Conventionally the reduction behavior of vanadia is analyzed by observing the peak appearance temperature of maximum hydrogen consumption ( $T_{\max}$ ), which increases as the reducibility decreases [37]. Therefore, as shown in Figure 7, the shift of  $T_{\max}$  to the low temperature indicates that the decrement of vanadium loading causes the formation of easily reducible vanadium state on catalyst [38,39].

As demonstrated in Figure 8(a), I compared H<sub>2</sub> TPR spectra for the 5 wt% and 7 wt% VT samples. It is notable that VT(4+) samples definitely show two distinct reduction peaks. These two low temperature and high temperature peaks arise from the

reduction of isolated and polymerized surface vanadium species on VT(4+) samples [40]. On the other hand, one reduction peak in H<sub>2</sub> TPR profile of VT(3+) and VT(5+) samples indicates that they exist mostly in polymerized vanadium form.

Moreover, the fact that T<sub>max</sub> of VT(3+) has shifted toward higher temperature implies that these vanadium species have less tendency to be reduced [36] because of the formation of highly coordinated polymeric vanadia species in VT(3+).

Additional evidence can be obtained from H<sub>2</sub> TPR results for 7 wt% VT (3+, 4+ and 5+) samples (Fig. 8(b)). It was clearly shown that 7 wt% VT(3+) sample contain most hardly reducible vanadia species, as confirmed by the position of T<sub>max</sub>. Such reduction behavior in VT(3+) samples is strongly related to the formation of highly polymerized vanadia species, which were probed by Raman (Figure 5) and UV–Vis results (Figure 6).

It can be summarized that a combination of Raman, UV–Vis and H<sub>2</sub> TPR results consistently provides the solid evidence of existence of highly coordinated polymeric vanadia species in VT(3+) samples.

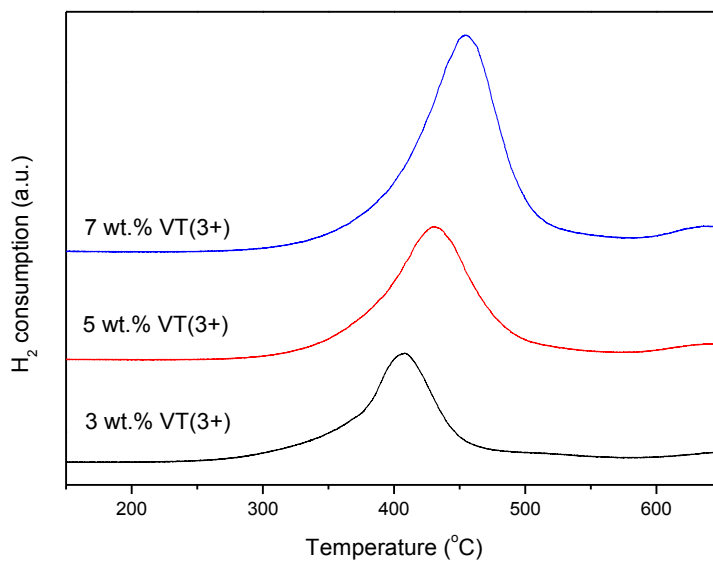


Figure 7. H<sub>2</sub> TPR profile of VT(3+) samples with different vanadium loading.

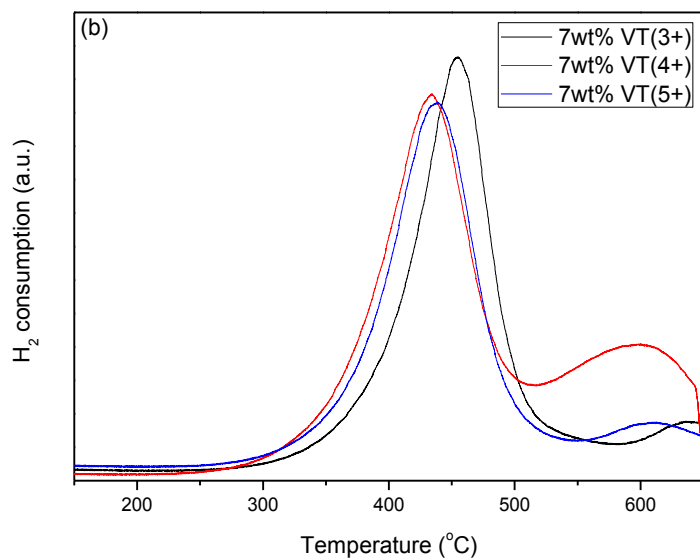
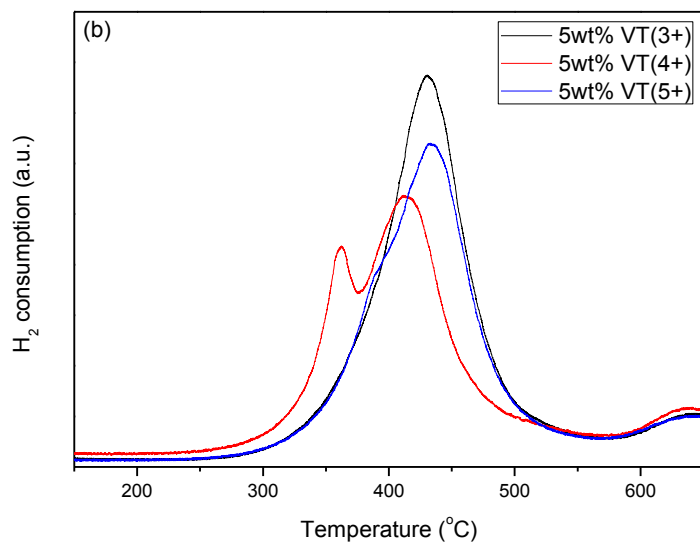


Figure 8. H<sub>2</sub> TPR profile of (a) 5 wt% VT (b) 7 wt% VT samples.

### 3.6. XPS

I use vanadium precursor with different oxidation states during the preparation of the catalysts. Therefore, XPS is employed to probe the oxidation states of vanadium oxide in VT samples [41].

Figure 9 presents V 2p X-ray photoelectron spectra of the VT(3+) samples. Although spectra of VT(4+) and VT(5+) are not shown in this paper, similar spectra are observed in other oxidation state samples. All vanadium species in the  $V_2O_5$  (3–7 wt%)/TiO<sub>2</sub> catalysts have V<sup>5+</sup> oxidation states (V 2p<sub>3/2</sub> = 517.5 eV) irrespective of the oxidation state of precursor solution, implying that the calcination at 400°C gives rise to the formation of V<sup>5+</sup> on these catalysts [11]. However, 1 wt% samples exhibit the V 2p<sub>3/2</sub> peak at 516.2 eV presenting the existence of V<sup>4+</sup> states [10,42,43]. Structural difference between 1 wt% and ≥ 3 wt% vanadium loading samples explains the dependence of vanadium oxidation state on the vanadium loading. This trend of dependence results in the completely different reaction behavior which will be covered later.

Table 3 demonstrates the relative surface concentration of V/Ti after calculating  $I_{V2p}/I_{Ti2p}$ . It clearly shows that V/Ti ratio increases with increasing the vanadium loading for all the samples [44], indicating that the surface coverage of vanadium on Ti increases. Also, the fact that V/Ti at the same vanadium loading is slightly lower for the samples prepared with low oxidation vanadium solution proposes that the VT(3+) samples

produce more aggregated vanadium species on  $\text{TiO}_2$  than VT(5+) ones except for 1 wt% samples.

It can be summarized that 1 wt% VT catalysts have different form of surface vanadium oxide ( $\text{V}^{4+}$ ) compared with other vanadium loaded samples and VT(3+) samples generate more aggregate form of vanadium oxide on  $\text{TiO}_2$ .

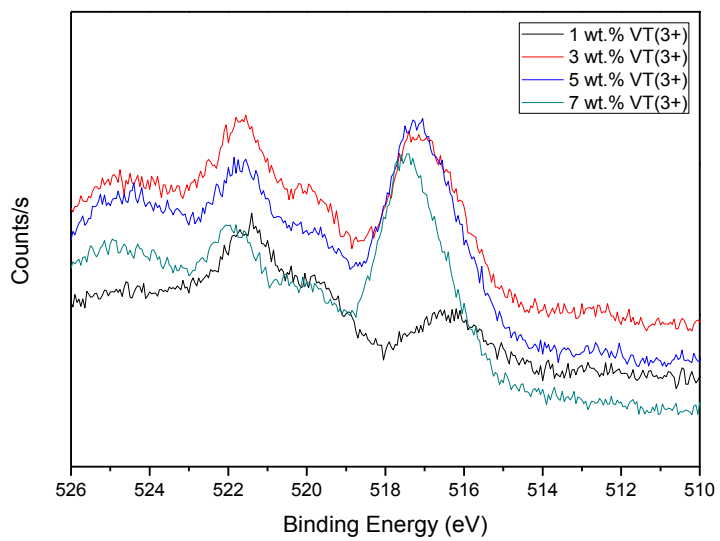


Figure 9. V 2p XPS spectra of VT(3+) samples.

Table 3. The relative surface concentration of V/Ti.

Sample		V/Ti ratio
VT(3+)	1wt%	0.092
	3wt%	0.132
	5wt%	0.159
	7wt%	0.184
VT(4+)	1wt%	0.095
	3wt%	0.101
	5wt%	0.156
	7wt%	0.191
VT(5+)	1wt%	0.087
	3wt%	0.259
	5wt%	0.271
	7wt%	0.357

### 3.7. NH<sub>3</sub>– SCR activity

Figure 10 shows the NO<sub>x</sub> conversion of all VT samples. It has to be pointed out that all 1 wt% VT samples show totally different reaction behavior compared with other vanadium loading samples, as indicated by the temperature of the maximum NO<sub>x</sub> conversion ( $T_{\max}$ ). It means that vanadium loading of catalyst has great influence on the  $T_{\max}$  during SCR reaction and active temperature range, resulting in the shift to the higher temperature region. However, irrespective of the oxidation states of vanadium precursor, catalysts with vanadium loading from 3 to 7 wt% have  $T_{\max}$  between at 250°C and at 300°C, while 1 wt% catalysts have maximum NO<sub>x</sub> conversion at higher temperature range (350–400°C). Such different tendency of NO<sub>x</sub> conversion behavior strongly suggests that two different vanadium species are formed depending on the vanadium loading on TiO<sub>2</sub>. This phenomenon was already confirmed by XPS result in Figure 9.

Even with increasing the vanadium loading from 3 wt% to 7 wt%, the active temperature window is shifted toward the lower temperature side. For example, 3 wt% VT samples have relatively lower activity below 250°C while 7 wt% VT ones. On the other hand, NO<sub>x</sub> conversion of 7 wt% VT significantly drops above 350°C where 3 wt% samples show much higher SCR activity. Therefore, it can be summarized that 5 wt% VT samples provide the optimum wide temperature window for NO<sub>x</sub> conversion as shown in Figure 11.

Previous research usually compared the catalyst as a function of NO<sub>x</sub> conversion [45–48], however, gas phase FT–IR makes it possible to further analyze about N<sub>2</sub>O yield. In the SCR catalysis, the incomplete reduction can produce unwanted products, N<sub>2</sub>O. Since N<sub>2</sub>O is known as a greenhouse gas which has 310 times greater influence on greenhouse effect than CO<sub>2</sub> [49], reducing the emission of N<sub>2</sub>O during SCR reaction also needs to be considered more seriously. As shown in Figure 12, I compare the amount of N<sub>2</sub>O produced over the samples. With increasing the amount of vanadium, the amount of N<sub>2</sub>O produced substantially increased especially at high temperature. When it comes to the comparison of N<sub>2</sub>O yield among the samples at the same vanadium loading (Figure 13), it is found that VT(3+) samples generate the least amount of nitrous oxide during SCR reaction.

It can be summarized that with respect to NO<sub>x</sub> conversion, N<sub>2</sub> selectivity and N<sub>2</sub>O production in outlet gas, 5 wt% VT(3+) catalyst demonstrates more desirable SCR performance (Figure 10, 11).

According to the study of Koranne et al. [36], the reduction of vanadia with NH<sub>3</sub> exhibited different behavior from that with H<sub>2</sub>. In other words, vanadium reduction induced by NH<sub>3</sub> preferred polymerized surface vanadium oxide species over the isolated surface vanadium oxide species in contrast to hydrogen reduction. Previous research claimed that polymeric species are 10 times more active than the monomeric species at low temperature around 200–250°C [50]. This phenomenon is

attributed to the higher lability of lattice oxygen atoms in polymeric vanadium species than in monomeric one, which results in faster reduction by  $\text{NH}_3$  and re-oxidation by gaseous oxygen [8].

As already shown in Figure 8(a), VT(4+) samples have both isolated and polymerized vanadium species on the support. While VT(3+) and VT(5+) samples show only one peak assigned to polymeric vanadium species.

the excellent reactivity of VT(3+) samples in  $\text{NH}_3$ -SCR reaction can be explained by the structural properties of vanadium oxide on  $\text{TiO}_2$  by combination of activity and characterization results [50]. VT(3+) catalysts have higher coordinated polyvanadate species are unambiguously proved by the multiple characterization results including Raman spectroscopy, UV-Vis DRS and  $\text{H}_2$  TPR. Accordingly, VT(3+) samples have more polymerized form of vanadium species on  $\text{TiO}_2$ , resulting in the highest performance of SCR catalysis.

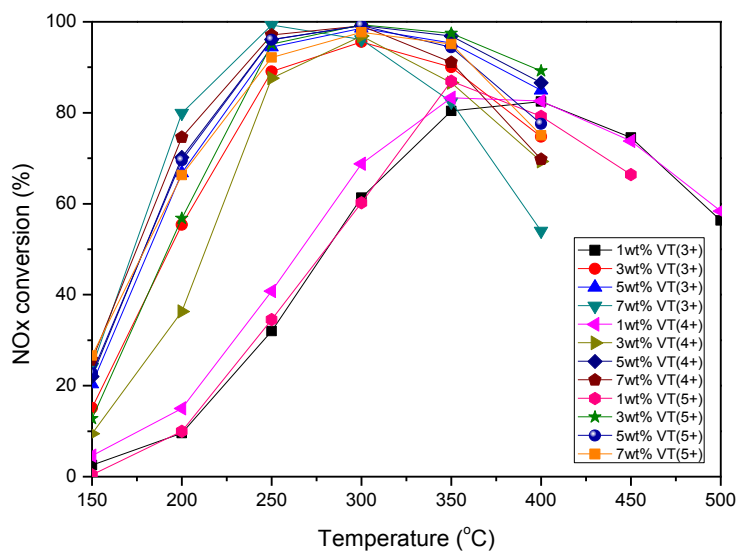


Figure 10. NOx conversion of all VT samples.

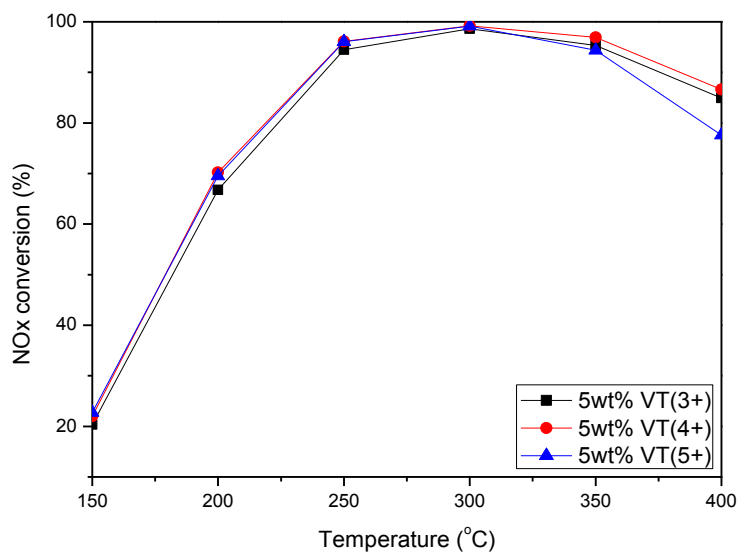


Figure 11. NOx conversion of 5 wt% VT samples.

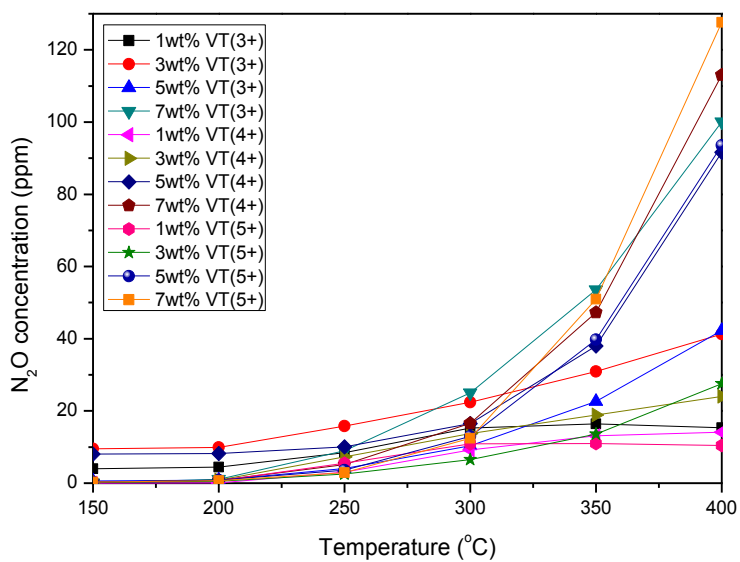


Figure 12. N<sub>2</sub>O concentration produced during SCR reaction of all VT samples.

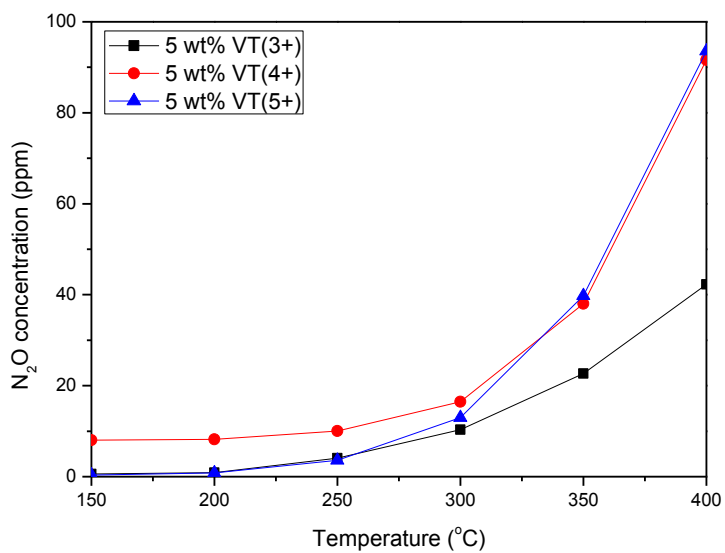


Figure 13. N<sub>2</sub>O concentration produced during SCR reaction of 5 wt% VT samples.

## Chapter 4. Conclusion

I investigated the effect of oxidation states of vanadium precursor solution of Vanadium catalysts on SCR reaction and analyze the physicochemical properties of  $V_2O_5/TiO_2$  catalysts. 5 wt% VT(3+) demonstrated the most desirable reaction behavior with the high NO<sub>x</sub> conversion in wide temperature range and N<sub>2</sub> selectivity, and lowest N<sub>2</sub>O formation during SCR reaction. A combined Raman, UV-Vis and H<sub>2</sub> TPR results clearly indicate that VT(3+) samples produce highly coordinated polymeric vanadia species. It was found that the physicochemical properties of vanadia species, especially the form of vanadyl species in catalysts, can be changed as a function of oxidation state of vanadium precursor solution, thus finally affecting the SCR reactivity.

## References

- [1] Denton, P. *et al.* "N<sub>2</sub>O as an intermediate for the formation of N<sub>2</sub> during SCR (NO): stationary and transient conditions". *Comptes Rendus de l'Académie des Sciences – Series IIC – Chemistry* **3**, 437–441, 2000.
- [2] Weng, R.–Y. & Lee, J.–F. "Catalytic performance and active sites determination of niobium oxide promoted vanadia/titania catalysts for selective catalytic reduction of nitric oxide". *Appl. Catal. A: Gen.* **105**, 41–51, 1993.
- [3] Martín, J. A., Yates, M., Ávila, P., Suárez, S. & Blanco, J. "Nitrous oxide formation in low temperature selective catalytic reduction of nitrogen oxides with V<sub>2</sub>O<sub>5</sub>/TiO<sub>2</sub> catalysts". *Appl. Catal. B: Environ.* **70**, 330–334, 2007.
- [4] Bosch, H. & Janssen, F. "Preface". *Catal. Today* **2**, v, 1988.
- [5] Zhu, Z. *et al.* "NO reduction with NH<sub>3</sub> over an activated carbon–supported copper oxide catalysts at low temperatures". *Appl. Catal. B: Environ.* **26**, 25–35, 2000.
- [6] Singoredjo, L., Slagt, M., van Wees, J., Kapteijn, F. & Moulijn, J. A. "Selective catalytic reduction of NO with NH<sub>3</sub> over carbon supported copper catalysts". *Catal. Today* **7**, 157–165, 1990.
- [7] Schneider, H., Maciejewski, M., Kohler, K., Wokaun, A. & Baiker, A. "Chromia Supported on Titania: VI. Properties of Different Chromium Oxide Phases in the Catalytic

- Reduction of NO by NH<sub>3</sub> Studied by in Situ Diffuse Reflectance FTIR Spectroscopy". *J. Catal.* **157**, 312–320, 1995.
- [8] Lietti, L. & Forzatti, P. "Temperature Programmed Desorption/Reaction of Ammonia over V<sub>2</sub>O<sub>5</sub>/TiO<sub>2</sub> De-NOxing Catalysts". *J. Catal.* **147**, 241–249, 1994.
- [9] Chiker, F., Nogier, J. P. & Bonardet, J. L. "Sub-monolayer V<sub>2</sub>O<sub>5</sub>-anatase TiO<sub>2</sub> and Eurocat catalysts: IR, Raman and XPS characterisation of VO<sub>x</sub> dispersion". *Catal. Today* **78**, 139–147, 2003.
- [10] Zhang, S. & Zhong, Q. "Promotional effect of WO<sub>3</sub> on O<sub>2</sub>- over V<sub>2</sub>O<sub>5</sub>/TiO<sub>2</sub> catalyst for selective catalytic reduction of NO with NH<sub>3</sub>". *J. Mol. Catal. A: Chem.* **373**, 108–113, 2013.
- [11] Silversmit, G., Depla, D., Poelman, H., Marin, G. B. & De Gryse, R. "Determination of the V2p XPS binding energies for different vanadium oxidation states (V<sup>5+</sup> to V<sup>0+</sup>)". *J. Electron Spectrosc. Relat. Phenom.* **135**, 167–175, 2004.
- [12] Magnusson, M., Fridell, E. & Ingelsten, H. H. "The influence of sulfur dioxide and water on the performance of a marine SCR catalyst". *Appl. Catal. B: Environ.* **111–112**, 20–26, 2012.
- [13] Smirniotis, P. G., Peña, D. A. & Uphade, B. S. "Low-Temperature Selective Catalytic Reduction (SCR) of NO with NH<sub>3</sub> by Using Mn, Cr, and Cu Oxides Supported on Hombikat TiO<sub>2</sub>". *Angew. Chem., Int. Ed.* **40**, 2479–2482,

- 2001.
- [14] Phil, H. H., Reddy, M. P., Kumar, P. A., Ju, L. K. & Hyo, J. S. "SO<sub>2</sub> resistant antimony promoted V<sub>2</sub>O<sub>5</sub>/TiO<sub>2</sub> catalyst for NH<sub>3</sub>-SCR of NO<sub>x</sub> at low temperatures". *Appl. Catal. B: Environ.* **78**, 301-308, 2008.
- [15] Agarwal, D. C., Nigam, P. C. & Srivastava, R. D. "Kinetics of vapor phase oxidation of methyl alcohol over supported V<sub>2</sub>O<sub>5</sub> K<sub>2</sub>SO<sub>4</sub> catalyst". *J. Catal.* **55**, 1-9, 1978.
- [16] Murakami, Y. *et al.* "Reaction mechanism of ammoxidation of toluene: I. Kinetic studies of reaction steps by pulse and flow techniques". *J. Catal.* **49**, 83-91, 1977.
- [17] Nakamura, M., Kawai, K. & Fujiwara, Y. "The structure and the activity of vanadyl phosphate catalysts". *J. Catal.* **34**, 345-355, 1974.
- [18] Mori, K., Miyamoto, A. & Murakami, Y. "Oxidation of furan on well-characterized vanadium oxide catalysts". *J. Catal.* **95**, 482-491, 1985.
- [19] Weckhuysen, B. M. & Keller, D. E. "Chemistry, spectroscopy and the role of supported vanadium oxides in heterogeneous catalysis". *Catal. Today* **78**, 25-46, 2003.
- [20] Bond, G. C. & Tahir, S. F. "Vanadium oxide monolayer catalysts Preparation, characterization and catalytic activity". *Appl. Catal.* **71**, 1-31, 1991.
- [21] Bruyère, V. I., Rodenas, L. A. G., Morando, P. J. & Blesa, M. A. "Reduction of vanadium (V) by oxalic acid in

- aqueous acid solutions". *J. Chem. Soc., Dalton Trans.*, 3593–3597, 2001.
- [22] Bruyère, V. I. E., Morando, P. J. & Blesa, M. A. "The Dissolution of Vanadium Pentoxide in Aqueous Solutions of Oxalic and Mineral Acids". *J. Colloid Interface Sci.* **209**, 207–214, 1999.
- [23] Hu, S. & Apple, T. M. "<sup>15</sup>N NMR Study of the Adsorption of NO and NH<sub>3</sub> on Titania-Supported Vanadia Catalysts". *J. Catal.* **158**, 199–204, 1996.
- [24] Richards, R. L. in *Encyclopedia of Inorganic Chemistry* (John Wiley & Sons, Ltd, 2006).
- [25] Choung, J. W., Nam, I.-S. & Ham, S.-W. "Effect of promoters including tungsten and barium on the thermal stability of V<sub>2</sub>O<sub>5</sub>/sulfated TiO<sub>2</sub> catalyst for NO reduction by NH<sub>3</sub>". *Catal. Today* **111**, 242–247, 2006.
- [26] Went, G. T., Leu, L.-j. & Bell, A. T. "Quantitative structural analysis of dispersed vanadia species in TiO<sub>2</sub>(anatase)-supported V<sub>2</sub>O<sub>5</sub>". *J. Catal.* **134**, 479–491, 1992.
- [27] Okuhara, T., Inumaru, K., Misono, M. & Matsubayashi, N. in *Stud. Surf. Sci. Catal.* Vol. Volume 75 (eds F. Solymosi L. Gucci & TÉTÉNYI P) 1767–1770 (Elsevier, 1993).
- [28] Griffith, W. P. & Lesniak, P. J. B. "Raman studies on species in aqueous solutions. Part III. Vanadates, molybdates, and tungstates". *J. Chem. Soc. A* **0**, 1066–1071, 1969.

- [29] Larrubia, M. A. & Busca, G. "An ultraviolet–visible–near infrared study of the electronic structure of oxide–supported vanadia–tungsta and vanadia–molybdena". *Mater. Chem. Phys.* **72**, 337–346, 2001.
- [30] Bañares, M. A. *et al.* "The Role of Vanadium Oxide on the Titania Transformation under Thermal Treatments and Surface Vanadium States". *J. Solid State Chem.* **124**, 69–76, 1996.
- [31] Srinivas, D. *et al.* "Active sites in vanadia/titania catalysts for selective aerial oxidation of  $\beta$ –picoline to nicotinic acid". *J. Catal.* **259**, 165–173, 2008.
- [32] Tang, F., Xu, B., Shi, H., Qiu, J. & Fan, Y. "The poisoning effect of Na<sup>+</sup> and Ca<sup>2+</sup> ions doped on the V<sub>2</sub>O<sub>5</sub>/TiO<sub>2</sub> catalysts for selective catalytic reduction of NO by NH<sub>3</sub>". *Appl. Catal. B: Environ.* **94**, 71–76, 2010.
- [33] Chary, K. V. R. *et al.* "The effect of zirconia polymorphs on the structure and catalytic properties of V<sub>2</sub>O<sub>5</sub>/ZrO<sub>2</sub> catalysts". *Catal. Today* **141**, 187–194, 2009.
- [34] Martínez–Huerta, M. V. *et al.* "Oxidative dehydrogenation of ethane to ethylene over alumina–supported vanadium oxide catalysts: Relationship between molecular structures and chemical reactivity". *Catal. Today* **118**, 279–287, 2006.
- [35] Held, A., Kowalska–Kuś, J. & Nowińska, K. "Epoxidation of propene on vanadium species supported on silica supports of different structure". *Catal. Commun.* **17**,

- 108–113, 2012.
- [36] Koranne, M. M., Goodwin, J. G. & Marcelin, G. "Characterization of Silica– and Alumina–Supported Vanadia Catalysts Using Temperature Programmed Reduction". *J. Catal.* **148**, 369–377, 1994.
- [37] Monaci, R. *et al.* "Oxidative dehydrogenation of propane over V<sub>2</sub>O<sub>5</sub>/TiO<sub>2</sub>/SiO<sub>2</sub> catalysts obtained by grafting titanium and vanadium alkoxides on silica". *Appl. Catal. A: Gen.* **214**, 203–212, 2001.
- [38] Matralis, H. K., Papadopoulou, C., Kordulis, C., Aguilar Elguezabal, A. & Cortes Corberan, V. "Selective oxidation of toluene over V<sub>2</sub>O<sub>5</sub>/TiO<sub>2</sub> catalysts. Effect of vanadium loading and of molybdenum addition on the catalytic properties". *Appl. Catal. A: Gen.* **126**, 365–380, 1995.
- [39] Lu, X. *et al.* "Selective oxidation of methanol to dimethoxymethane over acid–modified V<sub>2</sub>O<sub>5</sub>/TiO<sub>2</sub> catalysts". *Fuel* **90**, 1335–1339, 2011.
- [40] Wachs, I. E. & Weckhuysen, B. M. "Structure and reactivity of surface vanadium oxide species on oxide supports". *Appl. Catal. A: Gen.* **157**, 67–90, 1997.
- [41] Eberhardt, M. A., Proctor, A., Houalla, M. & Hercules, D. M. "Investigation of V Oxidation States in Reduced V/Al<sub>2</sub>O<sub>3</sub> Catalysts by XPS". *J. Catal.* **160**, 27–34, 1996.
- [42] Kasperkiewicz, J., Kovacich, J. A. & Lichtman, D. "XPS studies of vanadium and vanadium oxides". *J. Electron Spectrosc. Relat. Phenom.* **32**, 123–132, 1983.
- [43] Price, N. J., Reitz, J. B., Madix, R. J. & Solomon, E. I. "A

- synchrotron XPS study of the vanadia–titania system as a model for monolayer oxide catalysts". *J. Electron Spectrosc. Relat. Phenom.* **98–99**, 257–266, 1999.
- [44] Nogier, J. P., Jammul, N. & Delamar, M. "XPS study of TiO<sub>2</sub>–V<sub>2</sub>O<sub>5</sub> catalysts". *J. Electron Spectrosc. Relat. Phenom.* **56**, 279–295, 1991.
- [45] Oliveira, M. L. M. d. *et al.* "A study of copper–exchanged mordenite natural and ZSM–5 zeolites as SCR–NO<sub>x</sub> catalysts for diesel road vehicles: Simulation by neural networks approach". *Appl. Catal. B: Environ.* **88**, 420–429, 2009.
- [46] Chen, L., Li, J. & Ge, M. "The poisoning effect of alkali metals doping over nano V<sub>2</sub>O<sub>5</sub>–WO<sub>3</sub>/TiO<sub>2</sub> catalysts on selective catalytic reduction of NO<sub>x</sub> by NH<sub>3</sub>". *Chem. Eng. J. (Lausanne)* **170**, 531–537, 2011.
- [47] Huang, Y., Tong, Z.–q., Wu, B. & Zhang, J.–f. "Low temperature selective catalytic reduction of NO by ammonia over V<sub>2</sub>O<sub>5</sub>–CeO<sub>2</sub>/TiO<sub>2</sub>". *J. Fuel Chem. Technol.* **36**, 616–620, 2008.
- [48] Corbos, E. C. *et al.* "NO<sub>x</sub> abatement for lean–burn engines under lean–rich atmosphere over mixed NSR–SCR catalysts: Influences of the addition of a SCR catalyst and of the operational conditions". *Appl. Catal. A: Gen.* **365**, 187–193, 2009.
- [49] Government, E. (EPA Government, 2011).
- [50] Went, G. T., Leu, L.–J., Rosin, R. R. & Bell, A. T. "The

effects of structure on the catalytic activity and selectivity of V<sub>2</sub>O<sub>5</sub>/TiO<sub>2</sub> for the reduction of NO by NH<sub>3</sub>". *J. Catal.* **134**, 492–505, 1992.

# 요약(국문초록)

국제해사기구 (IMO)는 2016 년 이후 선박에서의 질소 산화물 (NO<sub>x</sub>) 배출에 관한 규제와 관련된 Tier III 를 시행할 예정이다. 선박에서의 선택적 촉매 환원 (SCR) 반응에 이용되는 촉매의 경우, 자동차에서 사용되는 SCR 촉매에 비해 저온 영역에서의 높은 활성을 필요로 한다. 이 논문에서는 저온 선택적 촉매 환원 반응의 촉매로 널리 알려진 V<sub>2</sub>O<sub>5</sub>/TiO<sub>2</sub> 촉매를 제조하는 과정에서, 바나듐 전구체 용액의 산화 상태를 변화시키며 최적의 반응을 나타내는 촉매를 연구하였다. Wet impregnation 방법을 이용하여 V<sub>2</sub>O<sub>5</sub>/TiO<sub>2</sub> (1, 3, 5, 7 wt%) 촉매를 제조하였으며 이 과정에서 V<sup>3+</sup>, V<sup>4+</sup> and V<sup>5+</sup> 총 세 가지 산화 상태를 갖는 바나듐 전구체 용액이 사용되었다. BET, ICP, XRD, Raman spectroscopy, UV-Vis DRS, H<sub>2</sub> TPR, XPS 분석을 통하여 제조한 촉매의 물리화학적 특성을 분석하였으며 또한, NH<sub>3</sub>-SCR 반응 실험을 진행하였다. 그 결과, V<sup>3+</sup>의 산화 상태를 갖는 바나듐 전구체 용액으로부터 제조된 바나듐 촉매 (VT(3+))가 넓은 온도 영역에서 좋은 활성을 나타냈으며, 선택적 촉매 환원 반응을 거치는 동안 가장 적은 양의 N<sub>2</sub>O 를 배출하였다. 높은 배위수를 갖는 바나듐 중합체를 형성됨으로 인하여 VT(3+) 촉매에서 가장 높은 NO<sub>x</sub> 전환율을 나타내고 N<sub>2</sub>O 가 적게 발생하는 것으로 판단된다.

주요어 : V<sub>2</sub>O<sub>5</sub>/TiO<sub>2</sub>, 산화상태, 바나듐 전구체, DeNO<sub>x</sub>, NH<sub>3</sub>-SCR

학 번 : 2012-20962